Matrix Isolation and ab Initio Studies of 1:1 Hydrogen-Bonded Complexes HCN−H_2O and HNC−H_2O Produced by Photolysis of Formaldoxime

Antti Heikkilä,* Mika Pettersson, Jan Lundell, Leonid Khriachtchev, and Markku Räsänen

Laboratory of Physical Chemistry, P.O. Box 55 (A. I. Virtasen aukio 1), University of Helsinki, FIN-00014 Helsinki, Finland

Received: October 27, 1998; In Final Form: February 8, 1999

The products of 193 nm photolysis of formaldoxime (CH_2NOH) are studied in solid argon at 17 K. Four species are experimentally found to appear in the photolysis, and they are identified with the aid of ab initio calculations as different HCN/HNC−water complexes: NCH···OH_2, HCN···HOH, CNH···OH_2, and HNC···HOH. The HNC−water complexes are experimentally observed for the first time. Computationally, the NCH···OH_2 complex possesses the lowest energy and the HCN···HOH complex is 5.3 kJ mol^{-1} higher in energy. The two HNC−water complexes are 60−70 kJ mol^{-1} higher in energy than the HCN−water complexes. The CNH···OH_2 is calculated to be the strongest complex with an interaction energy of about −30 kJ mol^{-1}. The barrier separating the HCN/HNC systems is high enough to prevent interconversion between them by IR pumping of the fundamental vibrations. On the other hand, rearrangement inside the two chemical systems is achievable with selective IR excitation of the OH, CH, and NH stretching vibrations.

1. Introduction

Hydrogen bonding is a widely explored area of physical chemistry.[1−8] The hydrogen-assisted interactions are important in atmospheric chemistry, catalytic reactions, surface chemistry, material science, and biological processes.

Water and hydrogen cyanide are well-known hydrogen bond formers, showing both proton donor and acceptor nature. The water dimer has typically been a model system of hydrogen bonding.[9] The capability of a water molecule to participate in up to four simultaneous hydrogen bonds forming infinite chains or three-dimensional solid lattices is of fundamental importance.[10,11] Hydrogen cyanide aggregates are of interest because the linear HCN subunit possessing a single lone electron pair can form linear chains of indefinite length.[6]

In the gas phase, the HCN−H_2O complex was studied by microwave spectroscopy in molecular beams.[12] The complex was deduced to have a vibrationally averaged, quasiplanar structure belonging to the C_{2v} point group. In this NCH···OH_2 complex, HCN donates a proton to the water oxygen. Turi and Dannenberg modeled this complex with semiempirical and ab initio calculations,[13] and their results agree with the structure reported in the gas phase.

The photochemical experiments on halogenated formaldoximes by Maier et al. suggest that there might be another hydrogen-bonded structure, i.e., a complex where water acts as a proton donor and the HCN nitrogen is a proton acceptor.[14] The CX_2NOH (X = Cl, Br) compounds decompose in rare gas matrixes, giving BrCN···HOBr and ClCN···HOCl hydrogen-bonded complexes. In these complexes, the hypohalogenous acid donates a proton to the nitrogen atom of BrCN or ClCN.

HNC was observed for the first time as a photoisomerization product of HCN in low-temperature rare gas matrixes[15] and later in interstellar space.[16] The HCN−HNC isomerization reaction was also studied experimentally.[17] Recently, Samuels and coworkers have computationally studied the thermochemistry of two hydrogen-bonded HCN−H_2O complexes and one HNC−H_2O complex.[18] The NCH···OH_2 complex was found to be more stable than HCN···HOH by 11.7 kJ mol^{-1} at the MP2/6-311G-(d,p) level of theory. The isomerization reaction between HCN and HNC was also studied, and the authors present only the HNC···HOH complex for hydrogen isocyanide. The HNC···HOH complex was calculated to be 90.1 kJ mol^{-1} higher in energy than the NCH···OH_2 complex.[18] However, no vibrational properties for the various complexes were reported.

In this paper, we report the vibrational spectrum of formaldoxime (CH_2NOH) in an argon matrix (17 K) and present the results of 193 nm photolysis of formaldoxime. Matrix isolation Fourier transform Infrared spectroscopy and ab initio methods are combined to study the photodecomposition products, and two different hydrogen-bonded structures of both HCN−H_2O and HNC−H_2O complexes are identified. The identification of the different isomers of the complexed species is aided by selective IR pumping of different vibrational transitions to induce internal reorganization of the complexes.

2. Experimental Details

Formaldoxime was generated from formaldoxime trimer hydrochloride salt (Merck, >98%), which was used without further purification. The hydrochloride salt was gently heated (ca. 50 °C) in a stainless steel tube continuously flushed with argon gas (AGA, ≥99.995%). Upon heating, the solid hydrochloride salt decomposes, releasing monomeric formaldoxime into the gas phase. The formaldoxime/Ar gas mixture was deposited onto a cooled CsI window in an Air Products HS-4 cryostat at 17 K. The preparation of monomeric CH_2NOH:Ar matrixes is complicated because the decomposition of the hydrochloride salt is highly sensitive to temperature. In the flushing technique used for depositing the samples, no exact matrix ratios could be determined, and monomericity was controlled by comparing the spectra obtained at different deposition conditions.

* Corresponding author. E-mail: Antti.Heikkila@csc.fi.

10.1021/jp984209z CCC: $18.00
Published on Web 04/02/1999

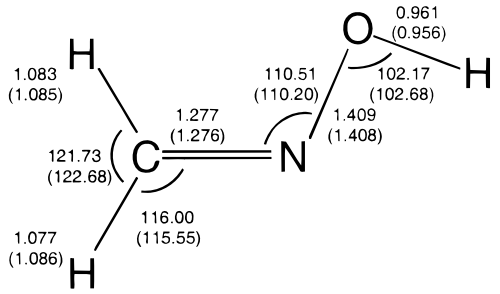

Figure 1. Calculated (MP2/6-311++G(2d,2p)) and experimental (in parentheses, from ref 21) structures of formaldoxime.

The IR spectra were recorded using a FTIR spectrometer (Nicolet 60 SX). Typically, 200 interferograms were coadded. The spectral resolution used was 1.0 cm^{-1} in the spectral region 400−4000 cm^{-1}.

The formaldoxime samples were photolyzed with an excimer laser (Estonian Academy of Sciences, ELI-76) operating at 193 nm (ArF). The pulse duration was 10 ns with pulse energies of ca. 10 mJ over the matrix surface (≈3 cm^2). Tunable pulsed IR radiation was provided by mixing the 1.06 μm radiation of a Nd:YAG laser (Powerlite 9010, Continuum) with the idler beam of an optical parametric oscillator (OPO Sunlite, Continuum) in a $LiNbO_3$ crystal. The pulse duration of the IR irradiation was ca. 5 ns with a line width of ∼0.1 cm^{-1}. A Burleigh WA-4500 wavemeter used to control the OPO radiation wavelength establishes an absolute accuracy better than 1 cm^{-1} for the IR radiation.

3. Computational Details

The Gaussian 94 program was used for the ab initio calculations.[19] All geometry optimizations and analytical frequency calculations were done at the MP2(FC)/6-311++G(2d,-2p) level after a set of preliminary scans of the complex potential energy surfaces at the HF−SCF level using various smaller basis sets. The interaction energies of the complexes were estimated using the CCSD(T)/6-311++G(2d,2p)//MP2/6-311++G(2d,-2p) level of theory. The interaction energies were corrected for the basis set superposition error (BSSE) by calculating the energy difference between the complex and the monomers in the complex basis (DCBS). This procedure corresponds to the counterpoise correction (CP) described by Boys and Bernardi.[20]

4. Experimental Results

IR Spectrum of Formaldoxime. Formaldoxime (CH_2NOH) is a planar molecule. Our ab initio geometry of formaldoxime and the experimental geometry obtained from microwave experiments[21] are presented in Figure 1. The comparison demonstrates a good agreement between the computational and experimental values.

The survey spectrum of formaldoxime in solid argon at 17 K is shown in Figure 2. The observed and identified absorption bands are collected in Table 1 and compared with our ab initio harmonic vibration frequencies and the gas-phase spectrum reported by Bannai.[22] The matrix shifts of the vibrations are generally small, the largest being 30 cm^{-1} downward in the OH-stretching mode. In solid argon, the ν_8 and ν_{11} bands split into multiplets. In the other bands splitting is not as clear, although shoulders can be seen. The origin of the splitting lies possibly in different trapping sites.

Photolysis of Formaldoxime. The 193 nm photolysis of formaldoxime in Ar is quite efficient and after ca. 2000 pulses all formaldoxime absorptions practically disappear. The IR absorptions generated under 193 nm laser irradiation are presented in Figure 3 and Table 2.

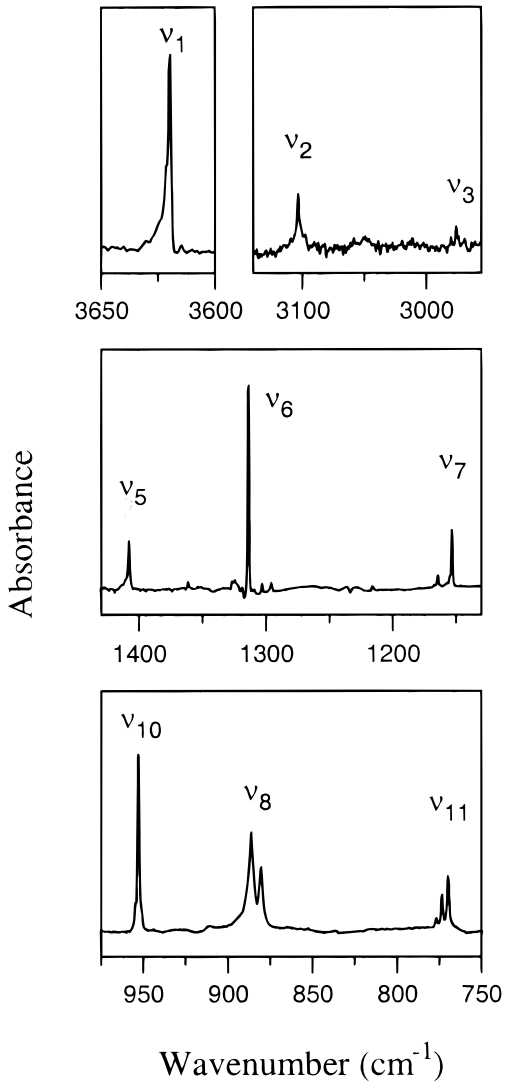

Figure 2. IR spectrum of formaldoxime (CH_2NOH) in solid Ar (17 K).

TABLE 1: Fundamental Absorptions of Formaldoxime in the Gas Phase[22] and in Solid Argon and Computational Frequencies and Intensities at the MP2/6-311++G(2d,2p) Level of Theory[a]

MP2/6-311++G(2d,2p)				
ω (cm^{-1})	I (km mol^{-1})	argon (cm^{-1})	gas phase (cm^{-1})	assignment
3707	102	3620	3650.3	ν_1 OH str
3163	1	3104	3109.7	ν_2 CH asymm str
3026	4	2976	2974.2	ν_3 CH symm str
1601	5	1624	1639.5	ν_4 CN str
1409	11	1408	1410.5	ν_5 CH_2 scissors
1294	78	1313	1319.0	ν_6 HON bend
1145	7	1151	1157.3	ν_7 CH_2 rock
935	38	954	952.6	ν_{10} CH_2 wag
876	107	886	892.6	ν_8 NO str
		880		
773	6	774	772.8	ν_{11} HON wag
		770		
513	7	526	530.0	ν_9 CNO bend
385	133		397.7	ν_{12} CNOH torsion

[a] The calculated frequencies are scaled with a constant factor of 0.96.

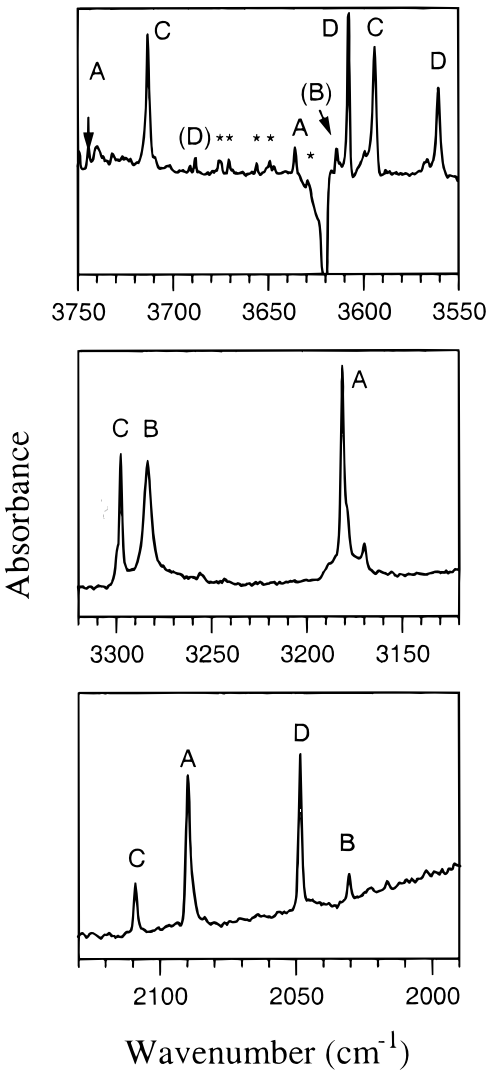

Figure 3. Difference spectrum demonstrating the results of 193 nm photolysis of formaldoxime. The formed species appear as positive absorptions; the formaldoxime bands correspond to negative absorptions. Ambient H_2O absorptions are marked with asterisks.

TABLE 2: Strongest Absorptions Observed after 193 nm Photolysis of Formaldoxime in Solid Argon at 17 K[a]

frequency (cm^{-1})	rel intensity	frequency (cm^{-1})	rel intensity
3713	32	2109	0.9
3608	9.6	2089	5.0
3594	22	2048	0.9
3560	7.4	2030	0.6
3298	22	813	13
3283	100	803	1.7
3181	50	727	18
		495	18

[a] The integrated intensities are scaled according to the strongest band observed (3282.1 cm^{-1}), which is given the value of 100.

The complexity of the recorded FTIR-spectrum immediately suggests the presence of several photoproducts. In fact, four different groups of absorptions can be recognized, and these are labeled as A−D in Figure 3. In particular, four distinct absorptions in the 2020−2110 cm^{-1} region suggest the presence of four different structures containing a C−N bond. The relative intensities of the observed absorptions change over a period of several hours after the photolysis, indicating that the photogenerated mixture of the new species is not in equilibrium. During overnight stabilization at 17 K, the bands marked with A and B increase and the bands marked with C and D decrease.

SCHEME 1

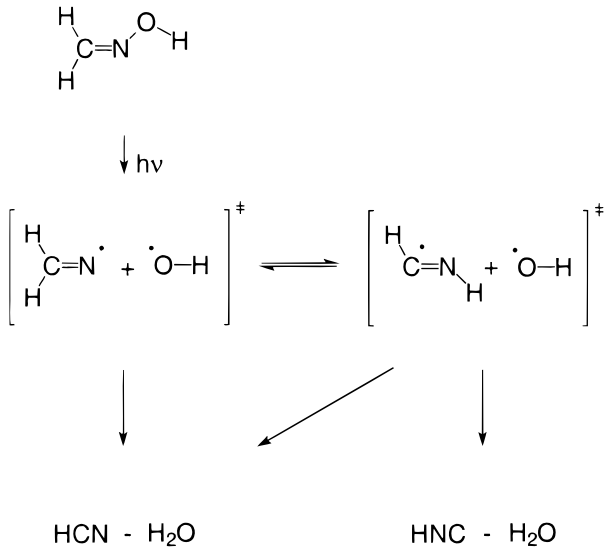

In the gas phase, formaldoxime has an absorption centered at 213 nm (n → π^*) and a strong absorption at 180 nm (π → π^*).[23] In the 193 nm photolysis of formaldoxime, OH radicals were observed.[24] Accordind to this, the primary excitation of formaldoxime at 193 nm in solid argon presumably produces a ($H_2CN^\bullet$ + $OH^\bullet$) radical pair in the cage, which can in secondary reactions form water and either HCN or HNC. In the photolysis of CH_2NOH in solid argon, no free HCN, HNC, $H_2CN^\bullet$, or $CN^\bullet$ is observed, indicating a strong cage effect. This resembles the photochemical decomposition of formic acid and formamide where the cage trapping was used to produce well-isolated 1:1 complexes H_2O−CO and NH_3−CO.[25−27] A possible mechanism for the production of H_2O and HCN or HNC is shown in Scheme 1.

The formation of H_2O and HCN can result from the reaction of OH radical with one of the hydrogen atoms of H_2CN, but the formation of HNC needs further explanation. The $H_2CN^\bullet$ radical formed in the photolysis might have enough excess energy to undergo a rapid rearrangement into HCNH by a hydrogen shift. The reaction between the C-bonded hydrogen and the $OH^\bullet$ radical can then produce HNC and H_2O. In fact, Bair and Dunning have studied the H_2CN−HCNH isomerization reaction with ab initio calculations. They found that *trans*-HCNH lies 58 kJ mol^{-1} higher in energy than H_2CN and the barrier for the isomerization is 219 kJ mol^{-1}.[28]

IR Excitation of the Photoproducts. The thermally relaxed samples were irradiated with narrow band IR radiation at different absorptions of the photolysis products. The irradiation selectively induces conversion of an irradiated species into another, as evidenced by the decrease of the irradiated set of bands and the increase of the other set. Two representative difference spectra are shown in Figure 4. The top trace presents the results of pumping at the 3181 cm^{-1} absorption of species A. When this band is pumped, the peaks labeled as A decrease while the bands labeled as C increase without changes in either B or D bands. After the IR pumping a dark interconversion from species C to A similar to the situation after photolysis of the formaldoxime precursor is observed. Pumping of any available band of species A above 3100 cm^{-1} produces species C and vice versa.

Pumping at the 3283 cm^{-1} absorption of species B increases the D absorptions and decreases the B absorptions, as shown in the lower trace of Figure 4. Irradiation of the other absorptions of B above 3100 cm^{-1} has the same effect. Similarly to the

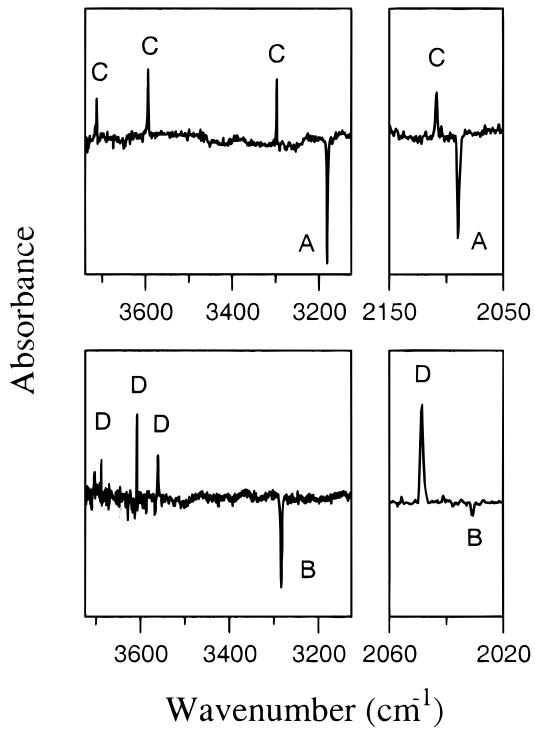

Figure 4. Two difference spectra demonstrating the results of OPO irradiation. The increasing species give positive absorptions, and the decreasing species give negative absorptions. The top trace shows the situation after IR pumping at 3181 cm^{-1}, and the lower trace applies to the situation after IR pumping at 3283 cm^{-1}.

species A and C, the thermal interconversion from D to B is observed after IR pumping of species B. Also, D can be converted to B by pumping the absorptions belonging to D. This suggests that species A and C are two different conformers of the same chemical system and that B and D are two conformers of the second chemical system produced from formaldoxime upon 193 nm photolysis. No interconversion from A or C to B or D was observed.

5. Hydrogen-Bonded Complexes HCN−H_2O and HNC−H_2O

To get a better insight on the H_2O−HCN and H_2O−HNC hydrogen-bonded complexes and to aid the interpretation of the experimental data obtained in low-temperature matrixes, we performed ab initio calculations for complexes of water with both HCN and HNC at the MP2/6-311++G(2d,2p) level of theory. We found four stable hydrogen-bonded complexes, which are presented in Figure 5. The structural parameters and calculated interaction energies of the HCN/HNC−H_2O complexes are collected in Tables 3 and 4. The calculated vibrational spectra of the complexes are collected in Table 5, and they are discussed below when the experimental bands are assigned to different complexes. Tables 3−5 and Figure 5 establish the following assignments for the experimentally observed bands: species A is NCH···OH_2, B is CNH···OH_2, C is HCN···HOH, and D is HNC···HOH.

Complex A (NCH···OH_2). The NCH···OH_2 complex has the lowest energy of the four complexes. The computational O−C distance, 3.128 Å, is close to the gas-phase experimental value of 3.152 Å.[12] The estimated interaction energy of the NCH···OH_2 complex is −19.39 kJ mol^{-1} at the CCSD(T) level with CP correction. Our MP2 value (−19.70 kJ mol^{-1}) does not differ significantly from the CCSD(T) value, which is probably due to the strength of the complex and the sufficiently

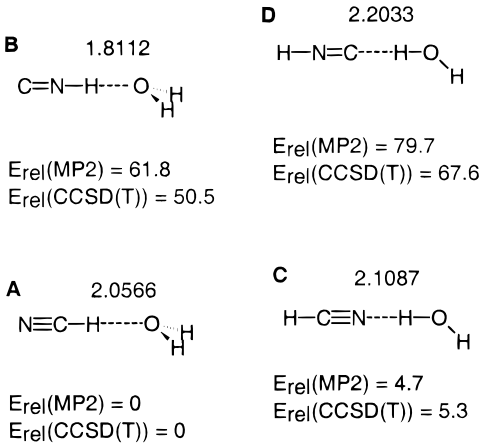

Figure 5. Hydrogen-bonded HCN−H_2O and HNC−H_2O complexes calculated at the MP2/6-311++G(2d,2p) level. The intermolecular distances of the complexes are expressed in angstroms, and the relative energetics are expressed in kJ mol^{-1} compared with the lowest energy species NCH···OH_2 (complex A), at the MP2 and CCSD(T) levels of theory.

flexible basis set used. The previous MP2 and semiempirical studies by Turi and Dannenberg also place this interaction energy at ca. −20 kJ mol^{-1}.[13]

For this complex, the calculations predict the following frequency shifts from free monomer values: +144 cm^{-1} for the HCN in-plane bending mode, +126 cm^{-1} for the HCN out-of-plane bending, −101 cm^{-1} for the CH-stretching and rather small shifts for the HOH bending, OH-stretching, and CN-stretching modes. Corresponding experimental shifts for bands of species A are +107 cm^{-1} for the HCN in-plane bending mode, +94 cm^{-1} for the HCN out-of-plane bending, and −122 cm^{-1} for the CH-stretching mode. The H_2O and CN-stretching modes are experimentally shifted by less than 10 cm^{-1}. The computational and experimental values are in good agreement with each other, which establishes the assignment of species A as the NCH···OH_2 complex. Out of the four complexes studied, this is the only one for which the computational frequencies fit the experimental values obtained for species A.

Complex C (HCN···HOH). In this complex, water is a proton donor, bonding with the nitrogen atom of HCN. Computationally, this complex is estimated to be 5.3 kJ mol^{-1} higher in energy than complex A at the CCSD(T) level. The counterpoise-corrected interaction energy for the HCN···HOH complex calculated at the CCSD(T) level is −14.41 kJ mol^{-1}. The weaker interaction is seen also as a small elongation of the intermolecular distance (2.1087 Å) compared with the lowest-energy NCH···OH_2 complex (2.0566 Å).

From the experimental point of view, distinguishing between the NCH···OH_2 and HCN···HOH complexes is straightforward. In the HCN..HOH complex, water is a proton donor, which causes large shifts to its OH-stretching and HOH-bending frequencies, and the CH-stretching mode of HCN should be relatively unperturbed upon complexation. The computational frequency shifts are −24 and −50 cm^{-1} for the OH-stretching modes and +23 cm^{-1} for the HOH bending. The CH-stretching and HCN-bending modes are predicted to shift by less than 10 cm^{-1} from the monomer values. In the experimental spectrum a group of similarly shifted bands labeled as C can be found: the OH-stretching bands shifted by −23 and −44 cm^{-1}, the HOH bending shifted by +38 cm^{-1}, the CH stretching shifted by −6 cm^{-1}, and the HCN in-plane and out-of-plane bendings shifted by +8 cm^{-1} and +7 cm^{-1}, respectively. The calculated shift for the C≡N-stretching mode of the HCN···HOH complex

TABLE 3. Geometrical Parameters[a] of the HCN−H_2O and HNC−H_2O Hydrogen-Bonded Complexes at the MP2/6-311++G(2d,2p) Level of Theory

	NCH···OH_2 (A)	CNH···OH_2 (B)	HCN···HOH (C)	HNC···HOH (D)
r(O−H_1)	0.9588	0.9592	0.9573	0.9572
r(O−H_2)			0.9629	0.9640
r(C−H_3)	1.0711		1.0637	
r(N−H_3)		1.0132		0.9964
r(C−N)	1.1669	1.1757	1.1646	1.1730
r(interaction)	2.0566	1.8112	2.1087	2.2023
∠(H_1−O−H_2)	104.88	105.30	104.26	104.25
∠(H_1−O−H_3)	125.15	119.71		
∠(H_2−O−H_3)	124.38	119.61		
∠(O−H_3−C)	179.86			
∠(O−H_3−N)		179.99		
∠(H_3−C−N)	179.96		179.89	
∠(H_3−N−C)		179.73		179.16
∠(O−H_2−C)				176.38
∠(O−H_2−N)			177.10	
∠(H_2−C−N)				173.25
∠(H_2−N−C)			171.32	
E_{el} (a.u.)	−169.5274111	−169.5038809	−169.5256141	−169.4970607

[a] Bond distances are given in Å, and bond angles, in degrees. The hydrogen atoms are numbered as follows: H_1 and H_2 hydrogens are the hydrogen atoms in the water molecule, H_1 being the noninteracting hydrogen and H_2 being involved in hydrogen bonding. H_3 is the hydrogen in either HCN or HNC.

TABLE 4. Calculated BSSE-Corrected Interaction Energies (in kJ mol^{-1}) of the HCN−H_2O and HNC−H_2O Complexes[a]

	NCH···OH_2 (A)	CNH···OH_2 (B)	HCN···HOH (C)	HNC···HOH (D)
MP2	−19.70	−32.38	−15.33	−16.28
MP3	−20.04	−30.63	−13.79	−14.42
MP4SDQ	−19.19	−29.70	−13.86	−14.46
CCSD	−19.14	−29.44	−13.69	−14.03
CCSD(T)	−19.39	−30.21	−14.41	−15.15

[a] The MP2/6-311++G(2d,2p) optimized structures are used in all single point energy calculations.

is +17 cm^{-1}, and the relative intensity of this mode is predicted to be small. In the experimental spectrum, a band attributed to species C according to the IR-pumping measurements can be found at 2109 cm^{-1}. This band shown in Figure 3 shifts by +15.9 cm^{-1} compared with the C≡N stretch in the HCN monomer and agrees with the calculated peak position.

The assignment of the HCN···HOH to species C perfectly agrees with our previous assignment of the H_2O···HCN complex. These two complexes represent the same chemical structure HCN−H_2O, and a relatively low barrier between them is natural. Indeed, we observed thermal C → A conversion and C ↔ A selective IR pumping, as discussed above.

Complex B (CNH···OH_2). When formaldoxime is photolyzed at 193 nm, formation of both HCN−H_2O and HNC−H_2O systems is energetically possible and the proposed channels are presented in Scheme 1. According to the calculations at the MP2/6-311++G(2d,2p) level, there are two stable HNC−H_2O complexes: CNH···OH_2 where HNC acts as a proton donor and HNC···HOH where HNC acts as a proton acceptor. These two structures are shown in Figure 5, and they are similar to the two HCN complexes. The transition state of HCN−HNC isomerization lies computationally 12 200 cm^{-1} (146 kJ mol^{-1}) higher in energy than HNC,[29] which explains the absence of IR-induced or dark (17 K) interconversion between HCN−H_2O and HNC−H_2O.

The CNH···OH_2 complex has some interesting features. The calculated intermolecular distance is very short (1.8112 Å) due to the strong interaction between the subunits. The interaction energy is estimated to be −30.21 kJ mol^{-1}. The strong interaction is also reflected in the NH bond distance, which grows to 1.0132 Å compared with the 0.9964 and 0.9961 Å, respectively, for HNC···HOH and monomeric HNC computed with the same method.

The large perturbations upon complexation can be observed in the calculated vibrational spectrum as well. The NH stretching band is predicted to shift by −304 cm^{-1} from the monomer value. The calculated relative intensity of this band is also very high: 1212 km mol^{-1}, which is 10-fold compared with all other vibrational intensities of this complex. The HNC bending modes are also strongly perturbed, calculated shifts being +393 cm^{-1} for the in-plane mode and +313 cm^{-1} for the out-of-plane mode. The OH-stretching modes are calculated to shift by −16 cm^{-1} for the antisymmetric mode and by −13 cm^{-1} for the symmetric mode. The other vibrations exhibit only small shifts upon complexation.

The calculated vibrational properties of the CNH···OH_2 complex fit well in the observed bands labeled as B. In this assignment, the experimental NH stretching band can be found at 3284 cm^{-1}, being shifted −336 cm^{-1} from the monomer absorption at 3620 cm^{-1}.[15] The HNC in-plane bending absorption is assigned at 819 cm^{-1} based on the IR-pumping experiments. This band is shifted +342 cm^{-1} from the monomer value. The out-of-plane bending mode is calculated to be 80 cm^{-1} lower and is experimentally found at 731 cm^{-1}, which is 88 cm^{-1} lower than the in-plane mode.

The OH-stretching modes are relatively unperturbed upon complexation, which complicates their assignment. A band at 3614 cm^{-1} is tentatively assigned to the symmetric OH-stretching mode, which is in agreement with the computational shift and intensity. However, the antisymmetric mode is obscured by uncomplexed water absorptions and cannot be detected. We assign the band at 2031 cm^{-1} to C−N stretching of complex B according to the IR-pumping experiments. This is the weakest band assigned to one of the complexes in the C−N stretching region, which correlates with the low calculated intensity as well.

Complex D (HNC···HOH). The HNC···HOH complex resembles the HCN···HOH complex. The calculated intermolecular distance is 2.2033 Å and the interaction energy is −15.15 kJ mol^{-1} at the CCSD(T) level. Substantial shifts are predicted for most of the vibrations of the HNC···HOH complex. It is

TABLE 5: Calculated and Experimental Frequencies of the HCN−H_2O and HNC−H_2O Complexes[a]

	exp freq ω (cm^{-1})	exp shift $\Delta\omega$ (cm^{-1})	calc freq ω (cm^{-1})	calc rel intensity I (km mol^{-1})	calc shift $\Delta\omega$ (cm^{-1})
			NCH···OH_2 (A)		
ν_1, ν_{as}(OH)	3740	+3.6	3812.6	100	−10.4
ν_2, ν_s(OH)	3635	−3.0	3699.5	19	−8.8
ν_3, ν(CH)	3182	−121.8	3220.2	351	−100.8
ν_4, ν(CN)	2090	−3.4	1933.5	9	−0.7
ν_5, δ(HOH)	1599	+8.2	1595.3	67	+0.5
ν_6, δ(HCN) in plane	827	+106.8	834.0	48	+144.2
ν_7, δ(HCN) oop	814,803	+94.1	815.9	40	+126.1
ν_8 intermolecular			243.1	75	
ν_9 intermolecular			144.6	69	
ν_{10} intermolecular			139.9	91	
ν_{11} intermolecular			101.6	118	
ν_{12} intermolecular			98.9	1	
			CNH···OH_2 (B)		
ν_1, ν_{as}(OH)			3806.9	114	−16.0
ν_2, ν_s(OH)	3614 (tentative)	−24.6	3695.6	22	−12.7
ν_3, ν(NH)	3284	−336.3	3364.5	1212	−303.9
ν_4, ν(CN)	2031	+11.8	1929.2	<1	−2.9
ν_5, δ(HOH)			1595.7	69	+0.9
ν_6, δ(HNC) in plane	819	+342.0	821.0	156	+393.4
ν_7, δ(HNC) oop	731	+254.0	740.2	149	+312.6
ν_8 intermolecular			286.2	18	
ν_9 intermolecular			227.1	219	
ν_{10} intermolecular			191.8	128	
ν_{11} intermolecular			119.3	9	
ν_{12} intermolecular			109.6	2	
			HCN···HOH (C)		
ν_1, $\nu_{non-bonded}$(OH)	3713	−22.7	3798.6	108	−24.4
ν_2, $\nu_{H-bonded}$(OH)	3594	−43.9	3658.6	98	−49.7
ν_3, ν(CH)	3298	−5.6	3323.7	83	+2.7
ν_4, ν(CN)	2109	+15.9	1951.5	<1	+17.2
ν_5, δ(HOH)	1629	+38.2	1617.9	94	+23.1
ν_6, δ(HCN)	728	+7.8	694.3	35	+4.5
ν_7, δ(HCN)	727	+6.8	694.1	40	+4.3
ν_8 intermolecular			459.7	113	
ν_9 intermolecular			272.2	97	
ν_{10} intermolecular			127.8	2	
ν_{11} intermolecular			61.6	64	
ν_{12} intermolecular			53.6	23	
			HNC···HOH (D)		
ν_1, $\nu_{non-bonded}$(OH)	3688 (tentative)	−47.9	3794.9	120	−28.1
ν_2, ν(NH)	3608	−12.0	3665.8	215	−2.6
ν_3, $\nu_{H-bonded}$(OH)	3560	−68.3	3632.4	361	−75.9
ν_4, ν(CN)	2048	+19.3	1954.7	26	+22.6
ν_5, δ(HOH)			1618.6	43	+23.7
ν_6, δ(HNC) in plane	498	+21.0	440.5	133	+12.9
ν_7, δ(HNC) oop	494	+17.0	439.0	130	+11.4
ν_8, intermolecular	487 (tentative)		501.3	107	
ν_9, intermolecular			290.0	96	
ν_{10}, intermolecular			125.5	2	
ν_{11}, intermolecular			67.7	56	
ν_{12}, intermolecular			64.7	27	

[a] Experimental shifts are calculated from literature monomer values.[15,30]

notable that the NH-stretching mode is estimated to have a higher frequency than the H-bonded OH-stretching mode. For the OH-, NH-, and CN-stretching modes, the computed and experimental values are in good agreement, as seen in Table 5. However, the HOH bending is obscured by overlapping water impurity absorptions, and it was not observed.

The experimental spectrum has a quartet around 490 cm^{-1}, which is assigned to complex D in the IR-irradiation experiments. This quartet consists of peaks at 498, 494, 491, and 487 cm^{-1} and might consist of both the HNC-bending modes and the intermolecular mode. The in plane and out-of-plane HNC-bending modes are predicted to shift by 11.5 and 13 cm^{-1} from the experimental monomeric HNC value of 477 cm^{-1}.[15] The calculations also predict a strong intermolecular mode at 501 cm^{-1}. Similarly to the HCN−H_2O complexes, the observed D→B dark process is in agreement with the calculated energetics, with B being the lower-energy form.

6. Conclusions

The products of 193 nm photolysis of formaldoxime are studied in low-temperature argon matrixes with FTIR technique. Four different species found after photolysis are identified as different structures of HCN/HNC−H_2O complexes. No monomeric HCN, HNC, or water was observed, which shows that the cage effect prevents exit of the primary photolysis products and that subsequent reactions lead to products with the stoichiometry of the precursor.

By using IR-pumping experiments and ab initio calculations at the MP2/6-311++G(2d,2p) level, the four experimental species are identified as hydrogen-bonded NCH···OH_2, HCN···HOH, CNH···OH_2, and HNC···HOH complexes, the HNC−H_2O complexes being observed for the first time. The NCH···OH_2 complex represents the lowest-energy species. The two HNC−H_2O complexes were estimated to be ca. 60−70 kJ mol^{-1} higher in energy than the two HCN−H_2O complexes, and the barrier separating HCN−H_2O from HNC−H_2O is sufficiently high to prevent interconversion by exciting the fundamental vibrations of the complexes. Computationally, the CNH···OH_2 is the strongest complex, the BSSE-corrected interaction energy being ca. −30 kJ mol^{-1} at the counterpoise-corrected CCSD(T)/6-311++G(2d,2p)//MP2/6-311++G(2d,2p) level. In all complexes, the subunits undergo strong perturbations upon complexation and the ab initio calculations agree with the experimental results. The two HNC−H_2O complexes and the two HCN−H_2O complexes can be interconverted with each other in a pairwise manner by selective pumping of the fundamental stretching modes of their subunits.

Acknowledgment. This work was supported in part by the Onnenmäki Foundation through their grant to A.H. The Academy of Finland is thanked for financial help made available to M.P. and J.L. The authors thank the CSC, Center for Scientific Computing Ltd. (Espoo, Finland), for generous computer mainframe time.

References and Notes

(1) Weber, H., Ed. *Structure and Dynamics of Weakly Bound Molecular Complexes*; Reidel: Dordrecht, The Netherlands, 1987.

(2) Hobza, P.; Zahradnik, R. *Intermolecular Complexes. The Role of van der Waals Systems in Physical Chemistry and Biodisciplines*; Elsevier: Amsterdam, 1988.

(3) Jeffrey, G. A.; Saenger, W. *Hydrogen Bonding in Biological Structures*; Springer-Verlag: Berlin, 1991.

(4) Belissent-Funel, M. C., Dore, J. C., Eds. *Hydrogen Bond Networks*; Kluwer: Amsterdam, 1994.

(5) Smith, D. A. *Modeling the Hydrogen Bond*; American Chemical Society: Washington, DC, 1994.

(6) Scheiner, S. *Hydrogen Bonding. A Theoretical Perspective*; Oxford University Press: New York, 1997.

(7) Hadzi, D., Ed. *Theoretical Treatments of Hydrogen Bonding*; Wiley: Chichester, U.K., 1997.

(8) van Duijneveldt-van de Ridjt, J. G. C. M.; van Duijneveldt, F. B. In Hadzi, D., Ed. *Theoretical Treatments of Hydrogen Bonding*; Wiley: Chichester, U.K., 1997.

(9) Xantheas, S. S. *J. Chem. Phys.* **1996,** *104*, 8821 and references therein.

(10) Suhai, S. *J. Phys. Chem*. **1995**, *99*, 1172.

(11) Jeffrey, G. A. *An Introduction to Hydrogen Bonding*; Oxford University Press: New York, 1997.

(12) Gutowsky, H. S.; Germann, T. C.; Augspurger, J. D.; Dykstra, C. E. *J. Chem. Phys.* **1992**, *96*, 5808.

(13) Turi, L.; Dannenberg, J. J. *J. Phys. Chem.* **1993**, *97*, 7899.

(14) Maier, G.; Bothur, A.; Eckwert, J.; Reisenauer, H. P.; Stump, T. *Liebigs Ann./Recueil* **1997**, 2505.

(15) Milligan, D. E.; Jacox, M. E. *J. Chem. Phys.* **1967**, *47*, 278.

(16) Snyder, L. E.; Buhl, D. *Bull. Am. Astron. Soc*. **1971,** *3*, 338.

(17) Maki, A. G.; Sams, R. L. *J. Chem. Phys*. **1981,** *75*, 4178.

(18) Samuels, A. C.; Jensen, J. O.; Krisnan, P. N.; Burke, L. A. *J. Mol. Struct. (THEOCHEM)* **1998,** *427*, 199.

(19) Frisch, M. J.; Trucks, G. W.; Schlegel, H. B.; Gill, P. M. W.; Johnson, B. G.; Robb, M. A.; Cheeseman, J. R.; Keith, T.; Petersson, G. A.; Montgomery, J. A.; Raghavachari, K.; Al-Laham, M. A.; Zakrzewski, V. G.; Ortiz, J. V.; Foresman, J. B.; Cioslowski, J.; Stefanov, B. B.; Nanayakkara, A.; Challacombe, M.; Peng, C. Y.; Ayala, P. Y.; Chen, W.; Wong, M. W.; Andres, J. L.; Replogle, E. S.; Gomperts, R.; Martin, R. L.; Fox, D. J.; Binkley, J. S.; Defrees, D. J.; Baker, J.; Stewart, J. P.; Head-Gordon, M.; Gonzalez, C.; Pople, J. A. *Gaussian 94*, revision E.2; Gaussian, Inc.: Pittsburgh, PA, 1995.

(20) Boys, S. F.; Bernardi, F. *Mol. Phys*. **1970**, *19*, 553.

(21) Levine, I. *J. Chem. Phys* **1963**, *38*, 2326.

(22) Bannai, R. A.; Duxbury, G.; Ritchie, G.; Klee, S. *J. Mol. Spectrosc*. **1996**, *178*, 84.

(23) Dargelos, A.; Sandorfy, C. *J. Chem. Phys*. **1977**, *67*, 3011.

(24) Dagdigian, P. J.; Anderson, W. R.; Sausa, R. C.; Miziolek, A. W. *J. Phys. Chem*. **1989**, *93*, 6059

(25) Lundell, J.; Räsänen, M. *J. Phys. Chem. A* **1995**, *99*, 14301.

(26) Lundell, J.; Räsänen, M. *J. Mol. Struct*. **1997**, *436*−*437*, 349.

(27) Lundell, J.; Krajewska, M.; Räsänen, M. *J. Phys. Chem. A* **1998**, *102*, 6643.

(28) Bair, R.; Dunning, T. *J. Chem. Phys*. **1985**, *82*, 2280.

(29) Pearson, P. K.; Schaefer H. F. *J. Chem. Phys*. **1975**, *62*, 350.

(30) Engdahl, A.; Nelander, B. *J. Mol. Struct*. **1989**, *193*, 101 and references therein.